

# 琉球大学学術リポジトリ

## Tomographic Resolution of URA Coded Aperture Imaging and Its Enhancement

メタデータ	言語: 出版者: 琉球大学工学部 公開日: 2007-09-16 キーワード (Ja): キーワード (En): 作成者: 陳, 延偉, 仲尾, 善勝 メールアドレス: 所属:
URL	<a href="http://hdl.handle.net/20.500.12000/1971">http://hdl.handle.net/20.500.12000/1971</a>

# Tomographic Resolution of URA Coded Aperture Imaging and Its Enhancement

Keisaku Kishimoto, Yen-Wei Chen, Zensho Nakao

## Abstract

Tomographic resolution of URA (uniformly redundant arrays) coded aperture imaging is studied quantitatively. The performance of URA camera for three-dimensional imaging is investigated and it is shown also that the tomographic resolution can be improved by the use of small pinholes for URA aperture and fine sampling for decoding.

## 1. Introduction

A number of coded aperture imaging (CAI) techniques have been used or proposed for X-ray imaging[1]. An advantage offered by the CAI lies in its large photon collection efficiency due to its large open area. Uniformly redundant arrays (URA)[2] is one of CAI techniques. In URA coded aperture imaging, a pinhole is replaced by multi-pinhole arrays arranged in *m-sequences*[3]. So the URA camera can provide a two-dimensional image with a high resolution and high SN ratio. Furthermore, since the URA camera can view the object with a large solid angle, it can also provide some tomographic resolution for a three-dimensional object[4,5]. In this paper, we make quantitative evaluation[6] of the tomographic resolution and propose a new method to enhance the tomographic resolution.

## 2. URA Coded Aperture Imaging

The basic concept of an URA coded aperture imaging is shown in Fig.1. The URA coded aperture imaging is a two-step technique. The first step is the coded image formation (encoding

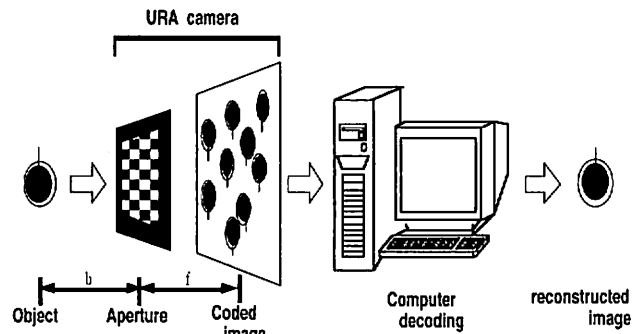


Fig.1 The basic concept of an URA coded aperture imaging.

process) and the second step is the reconstruction of the coded image with computer (decoding process). If the object is a planar (two-dimensional) object parallel to the aperture, the encoded image *P* is given by

$$P(k, l) = O * A = \sum_i \sum_j O(i, j) \cdot A(\text{mod}[i + k, r], \text{mod}[j + l, s]) \quad (1)$$

where *O* is an object distribution, *A* is the encoding operator describing the aperture function, and \* denotes the correlation operator. A reconstruction  $\hat{O}$  can be obtained by correlating a encoded image with the decoding operator *G* as

$$\begin{aligned} \hat{O}(i, j) &= P * G \\ &= \sum_k \sum_l P(k, l) \cdot G(\text{mod}[k + i, r], \text{mod}[l + j, s]) \quad (2) \\ &= (O * A) * G = O * (A * G) \end{aligned}$$

Received : 26 May, 1997

Department of Electrical and Electronic Engineering,  
Faculty of Engineering

This paper has been presented in ITC-CSCC'97

In order to obtain a perfect reconstruction ( $\hat{O} = O$ ),  $A * G$  must be a *delta function*. The key point of CAI is to find  $G$ , the correlational inverse of  $A$ . In URA, the auto-correlation  $\rho$  of  $m$ -sequences with an array of  $r \times s$  is given by

$$\rho = A * A = \begin{cases} (r \times s + 1) / 2; \text{ mod}(i, r) = 0 \text{ and } \text{mod}(j, s) = 0 \\ (r \times s + 1) / 4; \text{ otherwise} \end{cases} \quad (3)$$

The cyclic auto-correlation is a single value with a non-zero background. Furthermore, by defining a balanced operator by

$$\begin{cases} G(i, j) = 1; \text{ if } A(i, j) = 1 \\ G(i, j) = -1; \text{ if } A(i, j) = 0 \end{cases} \quad (4)$$

we can get a perfect delta function of  $A * G$  as

$$\hat{\rho} = A * G = \begin{cases} (r \times s + 1) / 2; \text{ mod}(i, r) = 0 \text{ and } \text{mod}(j, s) = 0 \\ 0; \text{ otherwise} \end{cases} \quad (5)$$

Thus we can obtain a perfect reconstruction with a  $(r \times s + 1) / 2$  times flux by using  $G$  as the decoding operator as shown in Eq(6). It means that the URA camera can provide an image with a high resolution and high SN ratio.

$$\hat{O} = O * (A * G) = \frac{(r \times s + 1)}{2} \cdot O \quad (6)$$

### 3. Performance of tomographic imaging

The basic concept of tomographic imaging with URA coded aperture is shown in Fig.2.

Sources distant to the detector cast smaller aperture shadows than closer sources. The size of the shadow depend on the distance to the point, while the location of the shadow depends on the lateral displacement of the point. By correlating the recorded image with decoding patterns of different sizes, images of the source distribution at different depths can be retrieved.

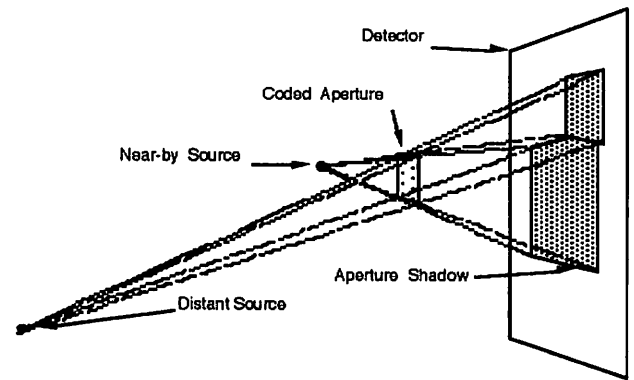


Fig. 2. The basic concept of tomographic imaging using URA coded aperture imaging.

The concept of the tomographic imaging can be expressed in simple mathematical terms[4,5]. Let  $P(x, y)$  be an encoded image at position  $(x, y)$  on the detector,  $O_z(x, y)$  be the distribution in a plane parallel to the aperture and a distance  $z$  from it, and let  $A_z(x, y)$  be the appropriately magnified version of the aperture for the distance  $z$ . There we have

$$P(x, y) = \sum_z [O_z(x, y) * A_z(x, y)] \quad (7)$$

that is, the recorded image is the sum of the correlation of each object plane with an aperture pattern of appropriate magnification.

To retrieve the  $z$ -th plane information from  $P(x, y)$ , one correlates it with a properly magnified decoding array  $G_z(x, y)$ , resulting in an estimate:

$$\begin{aligned} \hat{O}_z(x,y) &= P(x,y) * G_z(x,y) \\ &= \sum_z [O_z(x,y) * A_z(x,y)] * G_z(x,y) \quad (8) \\ &= O_z(x,y) + \sum_{z \neq z'} O_z(x,y) * [A_{z'}(x,y) * G_z(x,y)] \end{aligned}$$

Only one of the planes, the  $z$ -th, will be in focus, while all the others will be out of focus. Therefore, it is clear that if the second term of Eq (8) becomes zero, we can obtain a perfect reconstruction of  $z$ -th plane. Since usually  $A_{z'} * G_z$  is not a delta function, the second term appears on the  $z$ -th plane as a defocus artifact. The larger difference is between  $z$  and  $z'$ , the smaller is the defocus artifact.

We have carried out computer simulations to study the performance of tomographic imaging using URA camera. The simulated objects consist two planar objects  $O_1$  and  $O'_1$ , which are parallel to the aperture, as shown in Fig.3.

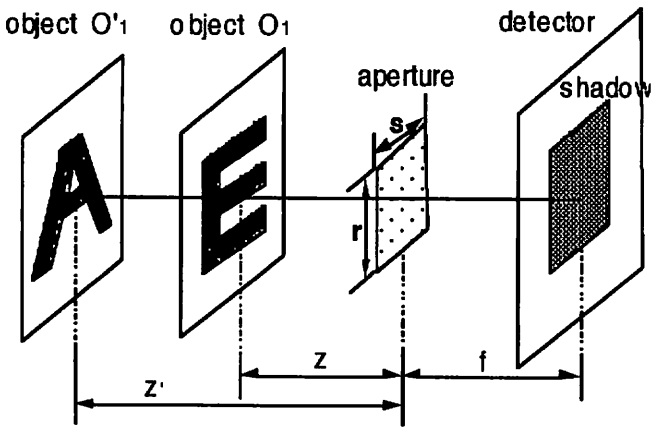


Fig. 3. An arrangement of URA camera for tomographic imaging

The aperture-object separations are  $z$  and  $z'$ . The magnifications for  $O_1$  and  $O'_1$  are  $M=f/z=5$  and  $M'=f/z'=4$ , respectively. The encoded image on the detector plane is the sum of the correlation of each object with an aperture pattern of appropriate

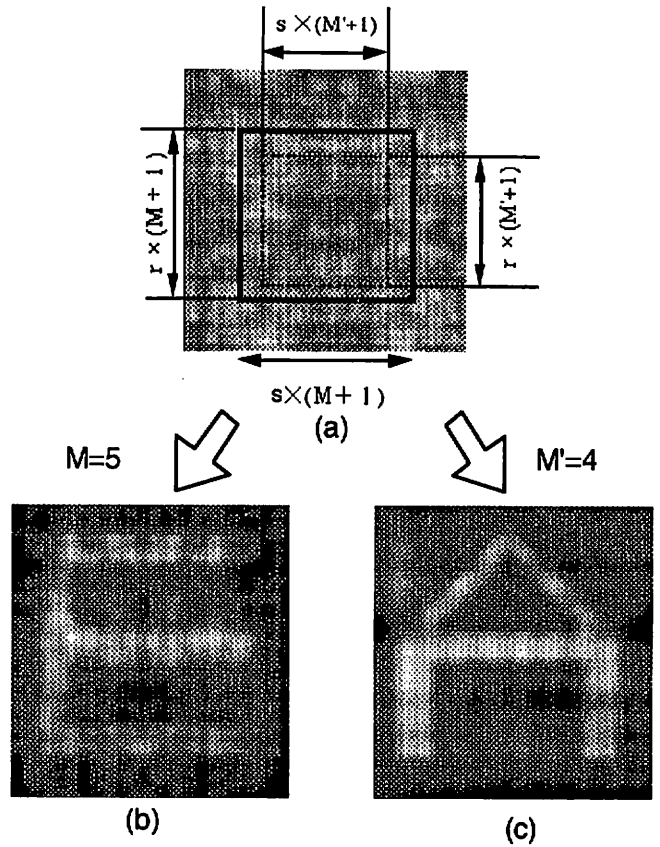


Fig. 4 (a) URA coded aperture image, (b) tomographic image of  $O_1$ , (c) tomographic image of  $O'_1$ .

magnification. The calculated encoded image is shown in Fig.4(a). The solid lines show the cyclic permutations of the basic aperture pattern with magnification  $M$  and  $M'$ . The URA coded aperture used in the simulation is of  $15 \times 17$ . By the use of the decoding patterns with the encoded images of different size  $r(M+1) \times s(M+1)$  for  $O_1$ ,  $r(M'+1) \times s(M'+1)$  for  $O'_1$ , images of  $O_1$  and  $O'_1$  at different depths are retrieved as shown in Fig.4(b) and 4(c). Though there are some defocus artifacts, the reconstructions of  $O_1$  and  $O'_1$  are clear.

In order to make quantitative evaluation, the depth point spread function (DPSF) was studied with a point-source. The point-source was assumed to be on axis with a source-aperture distance  $Z_0$ . The peak intensities of the reconstructed point-

source at different  $Z$  are shown in Fig.5. Figure 5 can be considered as the DPSF of the URA camera. The sharper is the DPSF, the higher is the tomographic (depth) resolution. The Tomographic resolution obtained is  $\Delta Z = 0.136Z_0$  for  $15 \times 17$  URA. If the source-aperture distance is 1 cm, the depth resolution is approximately 1.36 mm. This solution can be improved by the use of fine sampling and delta decoding.

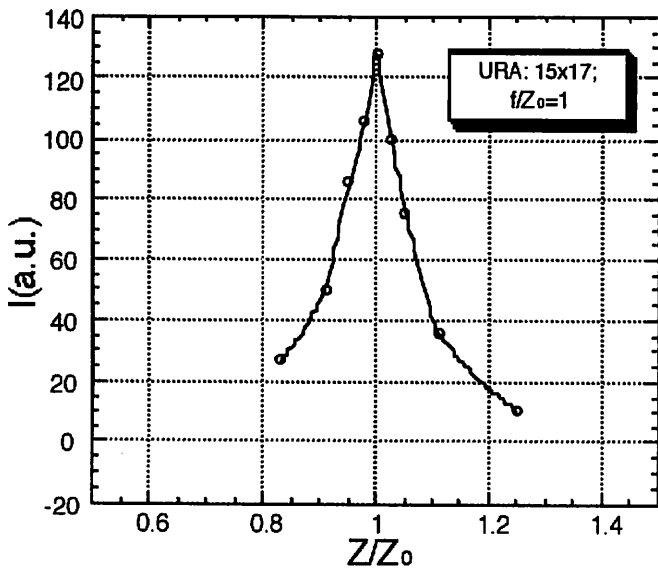


Fig.5 The depth point spread function.

4. Fine sampling and delta decoding

Let  $c$  be a size of one square element of URA pattern. Usually, a pinhole in URA aperture is smaller than  $c$  in size to have self-supporting. An example of the self-supporting pattern is shown in Fig.6. The pinhole size is  $c/4 \times c/4$ . Normal sampling and decoding patterns are shown in Figs.7(a) and 7(a'), respectively. There is no difference with that uses  $c \times c$  holes on the same URA function. The self-supporting pattern can be expressed with fine sampling[7]. Figures 7(b) and 7(b') show the computer array for the pattern

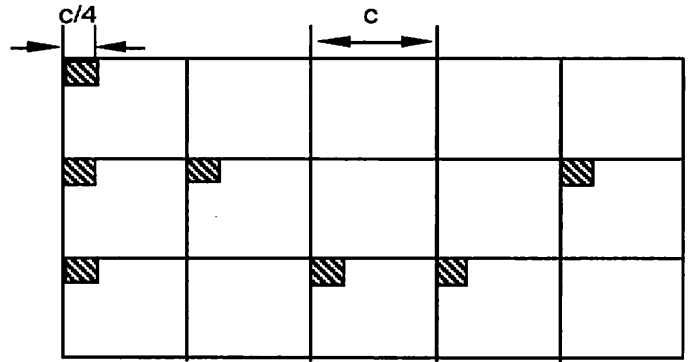


Fig.6 URA pattern (3 x 5) with self-supporting

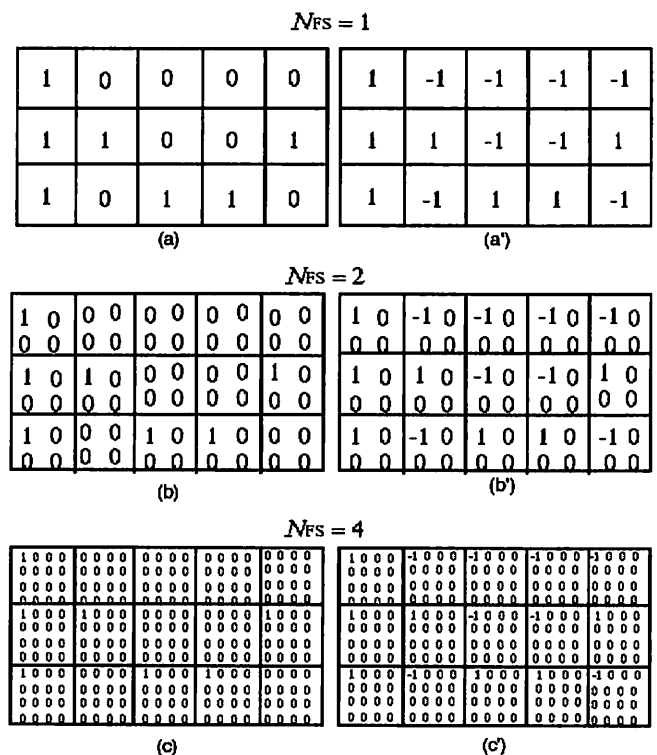


Fig.7 Assignment of values in the computer array for the URA patterns of Fig.6.

with  $N_{FS} = 2$ , and  $N_{FS} = 4$ , respectively, where  $N_{FS}$  is the number of fine sampling. The corresponding delta decoding patterns are shown Figs. 7(b') and 7(c'), respectively.

The results with different decoding patterns (Fig.7) are shown in Fig.8(a). The more is the number of fine sampling is increased, the sharper is the DPSF. Figure 8 shows that the tomographic resolution can be improved by the use of the fine

sampling and delta decoding method.

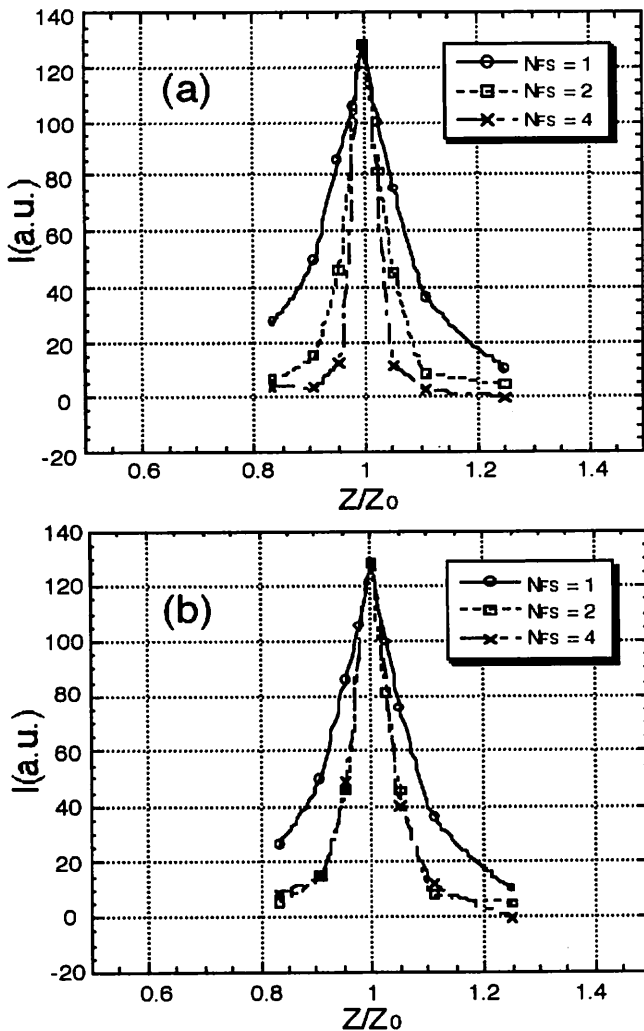


Fig. 8. The depth point spread function; (a) pinhole size= $c/4$ , (b) pinhole size= $c/2$ .

Furthermore, we show the results of URA aperture with pinhole of  $c/2$  in Fig.8(b). As in Fig.8(a), the tomographic resolution is improved by the use of fine sampling ( $N_{FS} = 2$ ), while there are no improvements of resolution for  $N_{FS} = 4$ . That means the tomographic resolution is determined by the pinhole size of the aperture. The smaller is the pinhole size, the better is the tomographic resolution. The dependance of the tomographic resolution on the pinhole size and the fine sampling is illustrated in Fig.9.

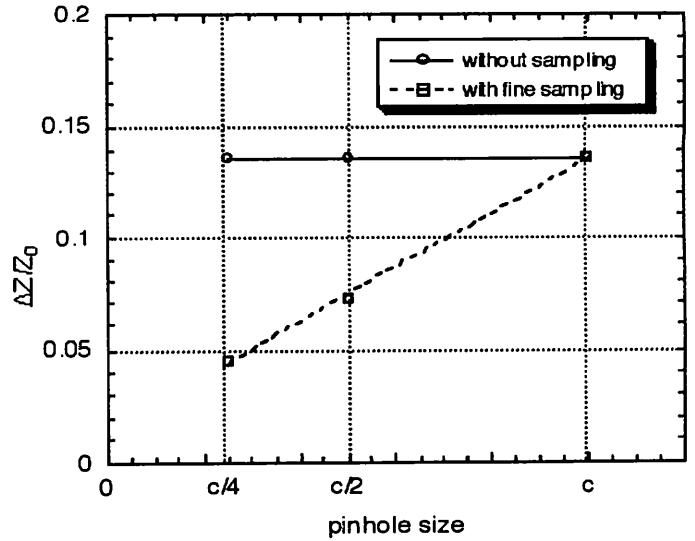


Fig.9. FWHM vs pinhole size

### 5. Summary

We investigated the performance of URA camera for three-dimensional imaging by simulation. The tomographic resolution of URA coded aperture imaging is quantitatively evaluated. We also show that the tomographic resolution can be improved using small pinholes for URA aperture and fine sampling for decoding.

### References

- [1] H.H Barrett and W.Swindell, *Radiological Imaging*, Academic Press, New York, 1981.
- [2] E.E.Fenimore and T.M.Cannon, "Coded aperture imaging with uniformly redundant arrays", *Appl. Opt.*, vol.17, no.3, pp.337-347, Feb. 1978.
- [3] M.Harwit and N.J.A.Sloane, *Hadamard Transform Optics*, Academic Press, New York, 1979.
- [4] E.E.Fenimore and T.M.Cannon, "Tomographical imaging using uniformly redundant arrays", *Appl. Opt.*, vol.18 no.7, pp.1052-1057,

April 1979.

[5] Y.-W.Chen et al., "Three-dimensional reconstruction of laser-irradiated targets using URA coded aperture cameras", *Opt. Comman.*, vol. 71, no. 5, pp.249-255, June 1989.

[6] K. Kishimoto, Y.-W. Chen et al., "A quantitative evaluation of URA coded aperture imaging", *Proc. ITC-CSCC'96*, Vol.1, pp.237-240, July 1996.

[7] E.E.Fenimore and T.M.Cannon, "Uniformly redundant arrays: digital reconstruction methods", *Appl. Opt.*, Vol.20 no.10, pp.1858-1864, May 1981.